Organometallics **1984**, *3*, 1879–1890

Probing Metal–Metal Bond Reactivity in a Series of Acetylene-Bridged Binuclear Complexes and the Structure of a Methyl Isocyanide Adduct, $[Rh_2Cl(CNMe)_2(\mu\text{-}CF_3C_2CF_3)(Ph_2PCH_2PPh_2)_2][BF_4]$

Martin Cowie,* Raymond S. Dickson, and Barry W. Hames

Department of Chemistry, The University of Alberta, Edmonton, Alberta, Canada T6G 2G2

Received April 12, 1984

The reactions of $[Rh_2Cl_2(\mu\text{-HFB})(DPM)_2]$ (1), $[Rh_2I_2(\mu\text{-HFB})(DPM)_2]$ (2), and $[Rh_2Cl_2(\mu\text{-DMA})(DPM)_2]$ (3) (HFB = hexafluoro-2-butyne, DMA = dimethyl acetylenedicarboxylate) with CO, SO_2, and CNMe have been investigated. With CO and SO_2 the complexes $[Rh_2X_2(\mu\text{-L})(\mu\text{-acetylene})(DPM)_2]$ (X = Cl, I; L = CO, SO_2) are obtained in which these ligands have inserted into the metal–metal bonds. The carbonyl group is more tightly bound than SO_2, and the iodo complex binds these groups stronger than the analogous chloro complex. These ligands are also more tightly bound when the accompanying bridging group is DMA instead of HFB. Reactions of compounds 1, 2, and 3 with CNMe proceed first by terminal attack to give the 1:1 adducts $[Rh_2X_2(CNMe)(\mu\text{-acetylene})(DPM)_2]$. Subsequent reaction with additional CNMe yields either $[Rh_2X(CNMe)_2(\mu\text{-acetylene})(DPM)_2][X]$ or $[Rh_2X_2(CNMe)_2(\mu\text{-acetylene})(DPM)_2]$, and further reaction yields $[Rh_2(CNMe)_4(\mu\text{-acetylene})(DPM)_2][X]_2$. The 1:1 and 2:1 adducts are each present in two isomeric forms whose relative abundance depends on the halide and the bridging acetylene groups present. No briding isocyanide groups are observed. The structure of one of the 2:1 adducts, as the BF_4^- salt $[Rh_2Cl(CNMe)_2(\mu\text{-HFB})(DPM)_2][BF_4]$ has been structurally characterized by X-ray techniques. This compound crystallizes in the space group $P2_1/n$ with $a = 16.366$ (3) Å, $b = 18.685$ (3) Å, $c = 20.425$ (4) Å, $\beta = 104.35$ (1)°, $V = 6051.1$ Å^3, and $Z = 4$. On the basis of 6800 unique observations and 367 parameters varied, the structure refined to $R = 0.059$ and $R_w = 0.097$. The complex has a bridging hexafluoro-2-butyne group, accompanying Rh–Rh bond, and a terminal Cl on one Rh center with two terminal CNMe groups on the other. This geometry is very similar to those proposed for the other isocyanide products.

Introduction

We have recently prepared the binuclear acetylene-bridged complex $[Rh_2Cl_2(\mu\text{-}CF_3C_2CF_3)(DPM)_2]$ (DPM = $Ph_2PCH_2PPh_2$) (1) and have shown, by an X-ray structure determination, that the acetylene group bridges the metals, bound as a cis-dimetalated olefin and accompanied by a Rh–Rh bond.[1] This complex closely resembles two other types of compounds previously studied in this group, namely, $[Rh_2X_2(\mu\text{-CO})(DPM)_2]$ (X = Cl, Br, I)[2-4] and $[Rh_2X_2(\mu\text{-}SO_2)(DPM)_2]$ (X = Cl, Br);[2,5] all three types of compounds are distorted A-frames having bridging π-acid groups, accompanying Rh–Rh single bonds, and terminal halide ligands.

One aspect of interest to us in these complexes regarded their possible Rh–Rh bond reactivities. $[Rh_2X_2(\mu\text{-CO})(DPM)_2]$ (X = Cl), for example, had been shown to undergo protonation at the Rh–Rh bond[6] while the three halo derivatives (X = Cl, Br, I) reacted with activated acetylenes with insertion of these groups into the Rh–Rh bond.[4] In contrast, neither the CO- nor the SO_2-bridged dihalides showed evidence of Rh–Rh bond reactivity with ligands such as CO, SO_2, or CNR but usually instead reacted to give complexes with these ligands bound terminally.[2,3,5,7] Complex 1, on the other hand, seemed a likely candidate for displaying metal–metal bond reactivity with ligands such as CO since the product of such a reaction would be exactly that compound obtained on reacting $[Rh_2Cl_2(\mu\text{-CO})(DPM)_2]$ with the activated acetylene $CF_3C_2CF_3$.[4] This also suggested that compound 1 may display metal–metal bond reactivity with other small groups such as CNR and SO_2.

We are also interested in the possibility of insertions of CO, CNR, and SO_2 into the Rh–acetylene bonds of species like compound 1. For these reasons a study was initiated to investigate the chemistry of compound 1, and related complexes, with small molecules such as CO, SO_2, and CNMe. The results of this study are reported herein.

Experimental Section

All solvents were purified according to standard procedures[8] and deaerated with a dinitrogen purge. Reactions were performed in Schlenk apparatus using inert-atmosphere techniques.[9] Sodium tetrafluoroborate (Alfa Inorganics), silver tetrafluoroborate (Aldrich), sulfur dioxide (Matheson), and carbon monoxide (Matheson) were used as received. $[Rh_2Cl_2(\mu\text{-}CF_3C_2CF_3)(DPM)_2]$ (1)[1] and methyl isocyanide[10] were prepared by the literature methods, and the purity of the isocyanide was ascertained by ^1H NMR spectroscopy. Infrared spectra were obtained as CH_2Cl_2 solutions in KCl cells or as Nujol mulls between either NaCl or KBr plates, using Nicolet MX-1 or 7199 FTIR spectrometers. NMR spectra were obtained at ambient temperature on Bruker WH-200 or WH-400 spectrometers or at −40 °C on a Bruker HFX-90 spectrometer. Conductivities of 1.00×10^{-3} M CH_2Cl_2 solutions were measured by using a Yellow Springs Instruments Model 31 conductivity bridge and 3401 cell.[11]

Preparation of $[Rh_2I_2(\mu\text{-}CF_3C_2CF_3)(DPM)_2]$ (2). A 200-mg (0.166-mmol) sample of compound 1 and 300 mg (1.81 mmol) of KI were placed in a flask under N_2, and 10 mL of CH_2Cl_2 and

---

[1] Cowie, M.; Dickson, R. S. *Inorg. Chem.* **1981**, *20*, 2682.

[2] Cowie, M.; Dwight, S. K. *Inorg. Chem.* **1980**, *19*, 2500.

[3] Cowie, M.; Dwight, S. K. *Inorg. Chem.* **1980**, *19*, 2508.

[4] (a) Cowie, M.; Southern, T. G. *J. Organomet. Chem.* **1980**, *193*, C46. (b) Cowie, M.; Southern, T. G. *Inorg. Chem.* **1982**, *21*, 246.

[5] (a) Cowie, M.; Dwight, S. K.; Sanger, A. R. *Inorg. Chim. Acta* **1978**, *31*, L407. (b) Cowie, M.; Dwight, S. K. *Inorg. Chem.* **1980**, *19*, 209.

[6] Sutherland, B. R.; Cowie, M. *Inorg. Chem.* **1984**, *23*, 1290.

[7] Cowie, M.; Gibson, J. A. E.; Dickson, R. S., unpublished results.

[8] Perrin, D. D.; Armarego, W. L. F.; Perrin, D. R. "Purification of Laboratory Chemicals"; Pergamon Press: Oxford, 1966.

[9] Shriver, D. F. "The Manipulation of Air-Sensitive Compounds"; McGraw-Hill: New York, 1969.

[10] Casanova, J.; Schuster, R. E.; Werner, N. D. *J. Chem. Soc.* **1963**, 4280.

[11] The conductivity cell was used in an inverted position, with the normal air exit vent sealed and a serum cap covering the open end. Typically, 20 mL of solution was used. The cell was calibrated by using 0.1 M KCl in H_2O.

0276-7333/84/2303-1879$01.50/0

Table I. Spectral Data for Reactions of Compounds 1, 2, and 3 with CO and SO_2

complex	$^{31}P\{^1H\}$ NMR[a] δ	$^{31}P\{^1H\}$ NMR[a] J,[b] Hz	infrared ν, cm^{-1} (assignt)
1, $[Rh_2Cl_2(\mu\text{-HFB})(DPM)_2]$	7.5	111.9	1642 (w) (C≡C)
2, $[Rh_2I_2(\mu\text{-HFB})(DPM)_2]$	9.1	110.0	1635 (w) (C≡C)
3, $[Rh_2Cl_2(\mu\text{-DMA})(DPM)_2]$	8.6	115.0	1615 (w) (C≡C) 1705 (br, m) (CO_2Me)
4, $[Rh_2Cl_2(\mu\text{-CO})(\mu\text{-HFB})(DPM)_2]$	8.9	131.8	1705 (m) (CO)
5, $[Rh_2I_2(\mu\text{-CO})(\mu\text{-HFB})(DPM)_2]$	9.5	131.0	1690 (m) (CO)
6, $[Rh_2Cl_2(\mu\text{-CO})(\mu\text{-DMA})(DPM)_2]$	11.0	140.6	1720 (m) (CO) 1660 (m) (^{13}CO) 1700 (br, m) (CO_2Me)
7, $[Rh_2Cl_2(\mu\text{-}SO_2)(\mu\text{-HFB})(DPM)_2]$	16.0	130.1	1140 (w), 1030 (w) (SO_2)
8, $[Rh_2I_2(\mu\text{-}SO_2)(\mu\text{-HFB})(DPM)_2]$	18.5	127.9	1128 (m), 1072 (w) (SO_2)
9, $[Rh_2Cl_2(\mu\text{-}SO_2)(\mu\text{-DMA})(DPM)_2]$	13.0	135.5	1162 (m), 1068 (w) (SO_2)

[a] Spectra were run on a Bruker HFX-90 spectrometer. [b] J is the splitting between the two major lines of AA'A''A'''X' spectra.[14]

10 mL of CH_3OH were added. The color of the suspension changed from green to dark brown within 15 min. This mixture was stirred overnight, and then most of the solvent was removed under a stream of N_2. The brown powder was dissolved in 10 mL of CH_2Cl_2, and the remaining KCl and KI were removed by two extractions with 10 mL of water. The H_2O and CH_2Cl_2 were removed by a dinitrogen stream, the residue was dried under vacuum, and the solid sample then was recrystallized from CH_2Cl_2/ether. The molar conductivity[12] of a 1.00 mM solution in CH_2Cl_2 was <0.4 Ω^{-1} cm^2 mol^{-1}, and the $^{31}P\{^1H\}$ NMR spectrum showed a resonance centered at 9.1 ppm with a splitting of 110.0 Hz between the two major lines. The ^{19}F NMR spectrum showed a sharp singlet at -50.0 ppm, while the infrared spectrum displayed a weak band at 1635 cm^{-1} attributable to the acetylenic C≡C stretch. Anal. Calcd for $Rh_2I_2P_4F_6C_{54}H_{44}$: C, 46.65; H, 3.19; F, 8.20; I, 18.25. Found: C, 46.51; H, 3.22; F, 8.03; I, 18.51.

Preparation of $[Rh_2Cl_2(\mu\text{-}CH_3OC(O)C_2C(O)OCH_3)(DPM)_2]$ (3). A 100-μL (0.813-mmol) sample of dimethyl acetylenedicarboxylate (DMA) was added to a flask containing 200 mg (0.406 mmol) of $[RhCl(C_8H_{12})]_2$[13] and 332 mg (0.810 mmol) of DPM under N_2. A 3.0-mL sample of CH_2Cl_2 was added immediately, whereupon the solution became dark green. After the solution was stirred for 15 min, 10 mL of ether was added to the suspension and the light green solid was filtered off. This sample was recrystallized from CH_2Cl_2/ether. The infrared spectrum showed an organic carboxylate stretch at 1705 cm^{-1} (br) and the stretch due to the coordinated acetylene moiety at 1615 cm^{-1}. The conductivity of a 1.00 mM CH_2Cl_2 solution was <0.4 Ω^{-1} cm^2 mol^{-1}, and the $^{31}P\{^1H\}$ NMR spectrum showed a resonance centered at 8.6 ppm with a separation of 115.0 Hz between the two major peaks. The ^1H NMR spectrum revealed a sharp singlet at 2.64 ppm attributable to the two equivalent DMA methyl groups as well as the DPM phenyl and methylene resonances in the appropriate regions (see Table II). Anal. Calcd for $Rh_2Cl_2P_4C_{56}H_{50}$: C, 56.64; H, 4.24; Cl, 5.97. Found: C, 56.03; H, 4.26; Cl, 6.14.

Reactions of Compounds 1, 2, and 3 with CO and SO_2. The reactions of the three acetylene-bridged complexes 1, 2, and 3 with CO to give 4, 5, and 6, respectively, were performed by syringing the appropriate volume of CO, at ambient temperature and pressure, into a solution or suspension of the starting complex in CH_2Cl_2. In a typical reaction this was carried out by adding 0.73 mL of CO (0.025 mmol) to 30 mg of compound 1 (0.025 mmol) in 3 mL of CH_2Cl_2 in a 10-mm NMR tube for acquiring the $^{31}P\{^1H\}$ NMR spectrum or by adding 0.25 mL of CO (0.0083 mmol) to 10.0 mg of compound 1 (0.0083 mmol) in 1.0 mL of CH_2Cl_2 in a 10-mL flask fitted with serum stoppers for observation of the solution infrared spectrum. Spectral results for these reactions are given in Table I.

The $^{31}P\{^1H\}$ NMR spectra of the reactions of compounds 1, 2, and 3 with 1 equiv of CO were observed at -40 °C, immediately after the injection of gas into the solution, which had been precooled to -40 °C, in attempts to observe possible intermediates. In all three cases the solutions darkened almost immediately, and the precipitation of considerable amounts of dark green or brown solids occurred within a few minutes. The $^{31}P\{^1H\}$ NMR spectra showed only the symmetric species 4, 5, and 6,[14] and the IR spectra of the isolated solids were identical with those previously reported for the complexes $[Rh_2X_2(\mu\text{-CO})(\mu\text{-acetylene})(DPM)_2]$.[4]

These reactions with 1 equiv of CO could not be reversed to any observable extent by flushing the solutions with a stream of N_2 at room temperature. Previous experiments with $[Rh_2Cl_2(\mu\text{-CO})(\mu\text{-HFB})(DPM)_2]$ (4) had shown that an overnight reflux in $CHCl_3$ with a slow N_2 purge was necessary to produce compound 1.[4] Similar conditions resulted in the loss of CO from 5 to yield 2, but refluxing $[Rh_2Cl_2(\mu\text{-CO})(\mu\text{-DMA})(DPM)_2]$ (6) for 48 h in $CHCl_3$ caused only partial reversal of this reaction; complete consumption of the complex required refluxing 200 mg of 6 in 50 mL of C_6H_6 with a slow N_2 purge for 2 1/2 days. However, under these conditions some $[Rh_2Cl_2(\mu\text{-CO})(DPM)_2]$ was also formed in addition to the expected compound $[Rh_2Cl_2(\mu\text{-DMA})(DPM)_2]$ (3).

The reactions of SO_2 with compounds 1 and 2 to give compounds 7 and 8, respectively, were performed by saturating CH_2Cl_2 solutions of the appropriate complex (100 mg in 5 mL), in 50- or 100-mL flasks, with SO_2. The initial green solutions turned dark brown almost immediately. After 48 h under an SO_2 atmosphere $^{31}P\{^1H\}$ NMR spectra were run at -40 °C and showed two symmetrical species in each case, one due to starting material and the other attributable to the SO_2 adduct (7 or 8). For the reaction yielding 7, about 15% remained as unreacted compound 1 and for 8 about 7% remained as 2, even under these conditions of high SO_2 concentration. Evaporation of these solutions by a nitrogen stream, followed by redissolving of the solids in CH_2Cl_2, revealed that only the respective starting materials remained.

The reaction of SO_2 with 3 was done in a manner similar to the reactions with CO; that is, 0.73 mL (0.028 mmol at ambient temperature and pressure) of SO_2 was injected into a solution of 30 mg(0.0253 mmol) of 3 in 1.5 mL of CH_2Cl_2 in a 10-mm NMR tube at room temperature. The green solution immediately turned a dark yellow-brown and a dark brown solid began precipitating after a few minutes. A $^{31}P\{^1H\}$NMR spectrum at -40 °C showed only a symmetrical pattern due to 9, which was the only product observed even with an excess of SO_2. A 20-min N_2 purge reversed the reaction to the extent that about 15% of compound 9 reverted to 3.

Due to the lability of the SO_2 ligand in compounds 7-9, they could not be isolated as pure solids. A summary of their $^{31}P\{^1H\}$ NMR and IR spectral details is given in Table I.

(c) Reactions of Compounds 1, 2, and 3 with CNMe. In a typical experiment 150 mg of compound 1 (0.124 mmol) was suspended in 0.7 mL of CD_2Cl_2 in a 5-mm NMR tube. Successive additions of 0.062 mL of a 1.0 M CD_2Cl_2 solution of the isocyanide (0.062 mmol) were made with NMR monitoring of the reaction

---

(12) For a normal 1:1 electrolyte, such as $[Rh_2(CO)_2(\mu\text{-Cl})(\mu\text{-CO})(DPM)_2][BPh_4]$, $\Lambda_M(10^{-3})$ = 45.8 Ω^{-1} cm^2 mol^{-1} in CH_2Cl_2.

(13) Chatt, J.; Venanzi, L. M. *J. Chem. Soc.* **1957**, 4735.

(14) the $^{31}P\{^1H\}$ NMR spectra appear as two major peaks with other minor peaks symmetrically disposed about the center of the pattern and are typical of an AA'A''A'''XX' spin system. See: Mague, J. T.; DeVries, S. H. *Inorg. Chem.* **1980**, *19*, 3743.

Table II. Spectral Data for Reactions of Compounds 1, 2, and 3 with CNMe

compd	NMR[a] δ			infrared
	^1H	^{19}F	$^{31}P\{^1H\}$	ν(CN), cm^{-1}
1, $[Rh_2Cl_2(\mu\text{-HFB})(DPM)_2]$[b]	7.03–7.62 (m, 40 H, C_6H_5), 3.59 (m, 2 H, CH_2), 2.92 (m, 2 H, CH_2)	−49.93 (s)	6.76 (112)	
10, $[Rh_2Cl_2(CNMe)(\mu\text{-HFB})(DPM)_2]$	3.32 (s, 3 H, CH_3)	−47.11 (11.5) (q), −47.88 (11.5) (q)	12.15 (122) (32), −0.11 (102) (36)	2192
11, $[Rh_2Cl_2(CNMe)(\mu\text{-HFB})(DPM)_2]$	2.98 (s, 3 H, CH_3)	−48.67 (br, s)	9.55 (124) (36), 2.67 (94) (36)	2212
12a, $[Rh_2Cl(CNMe)_2(\mu\text{-HFB})(DPM)_2][Cl]$	3.62 (s, 3 H, CH_3), 3.38 (s, 3 H, CH_3)	−47.62 (11.2) (q), −48.73 (11.2) (q)	11.67 (119) (34), 7.10 (87) (31)	2229, 2192
12b, $[Rh_2Cl(CNMe)_2(\mu\text{-HFB})(DPM)_2][BF_4]$	3.50 (s, 3 H, CH_3), 3.18 (br, 5 H, CH_2, CH_3)			2244, 2216
13a, $[Rh_2(CNMe)_4(\mu\text{-HFB})(DPM)_2][Cl]_2$	3.44 (sh, 6 H, CH_3), 3.04 (s, 6 H, CH_3)	−51.12 (s)	10.46 (90)	2216 (br)
13b, $[Rh_2(CNMe)_4(\mu\text{-HFB})(DPM)_2][BF_4]_2$	3.07 (sh, 6 H, CH_3), 3.06 (s, 6 H, CH_3)	−51.05 (s)	11.57 (89)	2234, 2217
2, $[Rh_2I_2(\mu\text{-HFB})(DPM)_2]$	6.97–7.70 (m, 40 H, C_6H_5), 4.14 (m, 2 H, CH_2), 3.22 (m, 2 H, CH_2)	−50.03 (s)	8.78 (110)	
14, $[Rh_2I_2(CNMe)(\mu\text{-HFB})(DPM)_2]$	3.44 (s, 3 H, CH_3)	−46.05 (11.6) (q), −47.03 (11.6) (q)	9.59 (119) (30), −0.16 (99) (30)	2182
15, $[Rh_2I_2(CNMe)(\mu\text{-HFB})(DPM)_2]$	2.94 (s, 3 H, CH_3)	−47.03 (11.0) (q), −47.83 (11.0) (q)	14.23 (92) (31), 6.21 (113) (32)	
16, $[Rh_2I(CNMe)_2(\mu\text{-HFB})(DPM)_2][I]$	3.59 (s, 3 H, CH_3), 3.37 (s, 3 H, CH_3)	−47.24 (11.1) (q), −48.62 (11.1) (q)	11.42 (119) (31), 7.69 (85) (31)	
17, $[Rh_2I_2(CNMe)_2(\mu\text{-HFB})(DPM)_2]$	2.89 (s, 6 H, CH_3)	−48.17 (s)	18.76 (93)	
13c, $[Rh_2(CNMe)_4(\mu\text{-HFB})(DPM)_2][I]_2$	3.07 (sh, 6 H, CH_3), 3.06 (s, 6 H, CH_3)	−51.05 (s)	11.57 (89)	2211 (br)
3, $[Rh_2Cl_2(\mu\text{-DMA})(DPM)_2]$	7.01–7.70 (m, 40 H, C_6H_5), 3.64 (m, 2 H, CH_2), 2.87 (m, 2 H, CH_2), 2.64 (s, 6 H, CH_3, (DMA))		8.07 (116)	
18, $[Rh_2Cl_2(CNMe)(\mu\text{-DMA})(DPM)_2]$	2.97 (s, 3 H, CH_3 (CNMe)), 2.74 (s, 3 H, CH_3 (DMA)), 2.26 (s, 3 H, CH_3 (DMA))		12.41 (127) (38), 3.71 (96) (38)	2196
19, $[Rh_2Cl(CNMe)_2(\mu\text{-DMA})(DPM)][Cl]$	3.62 (s, 3 H, CH_3 (CNMe)), 3.22 (s, 3 H, CH_3 (CNMe)), 2.81 (s, 3 H, CH_3 (DMA)), 2.41 (s, 3 H, CH_3 (DMA))		13.43 (120) (34), 10.21 (88) (33)	2235–2180
20, $[Rh_2(CNMe)_4(\mu\text{-DMA})(DPM)_2][Cl]_2$	3.68 (s, 6 H, CH_3 (CNMe)), 2.92 (s, 6 H, CH_3 (CNMe)), 2.77 (s, 6 H, CH_3 (DMA))		11.98 (94)	2201, 2218 (sh)

[a] Spectra were run on Bruker WH-400 spectrometer. [b] The slight differences between ^{31}P NMR parameters quoted here and those in Table I for compounds **1–3** result because of the different instruments used.

mixture after each addition. In this manner a series of NMR spectra was obtained ($^{31}P\{^1H\}$ at 161.92 MHz, ^{19}F at 376.41 MHz (for **1** and **2**), and ^1H at 400.14 MHz) for the reactions of compounds **1**, **2**, and **3** with CNMe over the range from 0 to 6 equiv of isocyanide per complex molecule. Typically, matching the $^{31}P\{^1H\}$, ^{19}F, and ^1H NMR signals arising from a given complex in the reaction sequence was straightforward on the basis of molecular symmetry, signal integration and amount of isocyanide added; where necessary all three spectra were obtained by using the same sample to confirm the assignments, which are given in Table II. Similar IR monitoring of the reaction sequence was carried out and, where possible, the isocyanide stretching frequencies were assigned (see Table II). The conductivities of 1.0 mM CH_2Cl_2 solutions of **1**, **2**, and **3** were also monitored as successive additions of CNMe were made.[15]

Preparation of $[Rh_2Cl(CNMe)_2(\mu\text{-HFB})(DPM)_2][BF_4]$ (12b). A 340-μL (0.35-mmol) sample of 1.04 M CNMe in CH_2Cl_2 was added with stirring to a suspension of 200 mg (0.166 mmol) of **1** in 10 mL of CH_2Cl_2 in a 100-mL three-necked round-bottom flask. A 5-mL sample of methanol was added to the green solution, followed by a solution of 100 mg (0.911 mmol) of $NaBF_4$ in 7 mL of methanol. A stream of N_2 was passed over the stirred solution for about 3 h, reducing its volume to about 8 mL and causing the precipitation of a purple microcrystalline solid. The light yellow supernatant was removed, and the solid was washed twice with 5 mL of methanol. A sample for elemental analysis was recrystallized from CH_2Cl_2/ether; it analyzed as a hemidichloromethane solvate (Calcd for $Rh_2Cl_2P_4F_{10}N_2C_{58.5}BH_{51}$: C, 50.79; H, 3.72; N, 2.02; Cl, 5.13. Found: C, 50.82; H, 3.69; N, 1.86; Cl, 4.98). A 200-MHz ^1H NMR spectrum of this solid in $CDCl_3$ solution confirmed the presence of dichloromethane. This spectrum also displayed resonances in the phenyl region (δ 6.9–8.0 (40 H, m)), one of two expected DPM methylene resonances (δ 3.72 (2 H, m)) and two singlets in the region appropriate for the isocyanide methyl protons. One of these singlets was superimposed on a broad multiplet, attributable to the other DPM methylene protons (δ 3.18 (5 H)), whereas the other was a sharp singlet (δ 3.50 (3 H)). An IR spectrum of **12b** as a Nujol mull revealed two isocyanide stretches at 2244 and 2216 cm^{-1}.

Preparation of $[Rh_2(CNMe)_4(\mu\text{-HFB})(DPM)_2][BF_4]_2$ (13b). The preparation of compound **13b** was similar to that for **12b**, except that 0.70 mL (0.73 mmol) of the 1.04 M CNMe solution was added to a suspension of 200 mg (0.166 mmol) of **1**. The resultant product was a yellow powder that was only slightly

---

(15) Supplementary material.

Table III. Summary of Crystal Data and Intensity Collection

compd	$[Rh_2Cl(MeNC)_2(\mu\text{-}CF_3C_2CF_3)(DPM)_2][BF_4]$
fw	1341.0
formula	$Rh_2ClP_4F_{10}N_2C_{58}BH_{50}$
space group	C_{2h}^5—$P2_1/n$ (nonstandard setting of $P2_1/c$)
cell parameters	
a, Å	16.366 (3)
b, Å	18.685 (3)
c, Å	20.425 (4)
β, deg	104.35 (1)
V, Å^3	6051.1
Z	4
d, g cm^{-3}	calcd 1.472, obsd 1.521 (by flotation)[a]
cryst dimens, mm	0.41 × 0.31 × 0.47
cryst shape	monoclinic prism with faces of the forms {010}, {011}, and {212}
cryst vol, mm^3	0.0125
temp, °C	23
radiation	Cu Kα
μ, cm^{-1}	65.407
range in abs correctn factors	0.258-0.417
receiving aperture, mm	3.5 × 4.5 (at 30 cm from crystal)
takeoff angle, deg	5.0
scan speed, deg min^{-1}	2.0 in 2θ
scan range, deg	1.00 below Kα_1 to 1.00 above Kα_2
bkgd counting times, s	10, 3° ⩽ 2θ ⩽ 60°; 20, 60° ⩽ 2θ ⩽ 78°; 40, 78° ⩽ 2θ ⩽ 120
2θ limits, deg	3 ⩽ 2θ ⩽ 120
unique data measd	9428
unique data used	6800
final no. of parameters varied	367
error in observn of unit weight (GOF)	2.009
R	0.059
R_w	0.097

[a] See the text for an explanation of the poor agreement between the observed and calculated densities.

soluble in methanol or methylene chloride. The ^{1}H NMR spectrum (see Table II) revealed the presence of four CNMe groups per complex molecule. Two isocyanide stretches were observed at 2234 and 2217 cm^{-1} in the IR spectrum of a CH_2Cl_2 solution of **13b**. Anal. Calcd for $Rh_2P_4N_4F_{14}C_{62}B_2H_{56}$: C, 50.51; H, 3.83; N, 3.80; Cl, 0.00. Found: C, 50.02; H, 3.88; N, 3.59; Cl, <1.

X-ray Data Collection on Compound 12b. Dark purple crystals of $[Rh_2Cl(CNMe)_2(\mu\text{-}HFB)(DPM)_2][BF_4]$ (**12b**) were obtained by slow diffusion of diethyl ether into a CH_2Cl_2 solution of the complex. A suitable crystal was mounted on a glass fiber. Preliminary film data showed that the crystal belonged to the monoclinic system and had systematic absences (*h*0*l*; *h* + l odd; 0*k*0; *k* odd) characteristic of the space group $P2_1/n$, a nonstandard setting of $P2_1/c$. Accurate cell parameters were obtained by a least-squares analysis of the setting angles of 12 carefully centered reflections chosen from diverse regions of reciprocal space (50° ≤ 2θ ≤ 60°, Cu Kα radiation) and obtained by using a narrow X-ray source. See Table III for pertinent crystal data and details of intensity collection. The widths at half-height of several strong low-angle reflections (ω scan, open counter) lay in the range 0.20–0.26°. Data were collected on a Picker four-circle automated diffractometer equipped with a scintillation counter and a pulse-height analyzer tuned to accept 90% of the Cu Kα peak. Background counts were measured at both ends of the scan range with both crystal and counter stationary. The intensities of three standard reflections were measured every 100 reflections during the data collection, and a second set of four standards was monitored twice a day. No significant decay of these standards was observed over the course of the data collection. The intensities of 9428 unique reflections (3° ≤ 2θ ≤ 120°) were measured and processed in the usual way, using a value of 0.05 for *p*.[16] Of these 6800 had $F_o^2 \geq 3\sigma(F_o^2)$ and were used in subsequent calculations. Absorption corrections were applied to the data using Gaussian integration.[17]

Structure Solution and Refinement. The structure was solved by using a sharpened Patterson synthesis to locate the two independent Rh atoms. Subsequent refinements and difference Fourier syntheses led to the location of all atoms of the anion and cation including hydrogens. Atomic scattering factors were taken from Cromer and Waber's tabulation[18] for all atoms except hydrogen, for which the values of Stewart et al.[19] were used. Anomalous dispersion terms[20] for Rh, Cl, and P were included in F_c. The carbon atoms of all phenyl rings were refined as rigid groups having D_{6h} symmetry and 1.392 Å C–C distances but with independent isotropic thermal parameters. All hydrogen atoms located were included as fixed contributions and were not refined. The idealized positions of the phenyl and methylene hydrogens were calculated from the geometries about the attached carbon atom by using C–H distances of 0.95 Å. The methyl hydrogens were located approximately from difference Fourier maps and then idealized such that the methyl carbon atoms had C_{3v}, symmetry with C–H bond lengths of 0.95 Å. All other nongroup atoms were refined independently with anisotropic thermal parameters. Since the geometry of the tetrafluoroborate anion appeared to be irregular and its fluorine atoms all exhibited larger thermal parameters, these atoms were removed from the refinements. However, a subsequent difference Fourier map, phased on the model without these atom contributions, reaffirmed their positions and showed the rather diffuse nature of the peaks. These atoms were reinserted, and refinement was continued as previously. At this time a region of electron density (0.99–2.33 e Å^{-3}) was located remote from the anion or complex cation. Although both CH_2Cl_2 and Et_2O were observed in ^{1}H NMR spectra of the solid redissolved in $CDCl_3$ and the presence of CH_2Cl_2 was suggested by the elemental analysis, all attempts to assign the electron density to disordered CH_2Cl_2, Et_2O, or both were unsuccessful. In all attempts, the peaks did not fit any simple disorder pattern, yielding chemically unreasonable geometries and badly behaved thermal parameters. In any case, the refinements involving the various disordered solvent models did not cause a significant change in the parameters associated with either the anion or cation as compared to the results in refinements without these disordered groups so this electron density was left unaccounted for in subsequent refinements. In the final difference Fourier map the top five residual peaks (0.99–2.33 e Å^{-3}) were associated with the assumed disordered solvent molecules and the next 20 (0.46–0.94 e Å^{-3}) were in the vicinities of the metals, the tetrafluoroborate anion, and the phenyl rings. A typical carbon atom on earlier Fourier syntheses had a peak intensity of ca. 2.9 e Å^{-3}. The final model with 367 parameters varied converged to $R = 0.059$ and $R_w = 0.097$.[21] No doubt the refinement suffers from our inability to adequately assign the portion of electron density that we assume corresponds to disordered solvent. The absorption coefficient used was the one assuming no solvent was present. With partial occupancy of solvent (as suggested by crystal density measurements and the elemental analysis) the absorption coefficient is not sufficiently different to result in a significant variation in the correction applied so should produce no adverse effects in the refinements.

The final positional and isotropic thermal parameters of the non-hydrogen atoms and the group atoms are given in Tables IV and V, respectively. Other data are available.[15]

Description of Structure of Compound 12b. A perspective view of the cation together with the numbering scheme is shown in Figure 1 (phenyl hydrogens have the same number as their

---

[16] Doedens, R. J.; Ibers, J. A. *Inorg. Chem.* **1967**, *6*, 204.

[17] See ref 1 for the programs used in solution and refinement of the structure.

[18] Cromer, D. T.; Waber, J. T. "International Tables for X-ray Crystallography"; Kynoch Press: Birmingham, England, 1974; Vol. IV, Table 2.2.A.

[19] Stewart, R. F.; Davidson, E. R.; Simpson, W. T. *J. Chem. Phys.* **1965**, *42*, 3175.

[20] Cromer, D. T.; Liberman, D. *J. Chem. Phys.* **1970**, *53*, 1891.

[21] $R = \Sigma||F_o| - |F_c||/\Sigma|F_o|$; $R_w = [\Sigma w(|F_o| - |F_c|)^2/\Sigma wF_o^2]^{1/2}$.

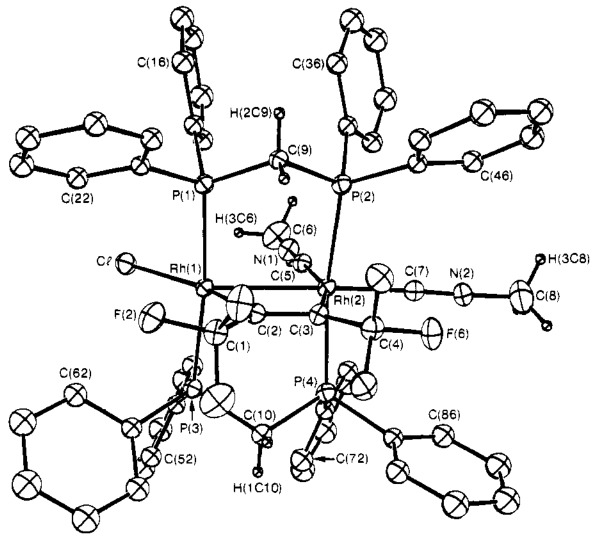

Figure 1. A perspective view of the $[Rh_2Cl(CNMe)_2(\mu\text{-HFB})(DPM)_2]^+$ cation showing the numbering scheme used. The 20% thermal ellipsoids are used except for the hydrogen atoms, which are drawn artifically small.

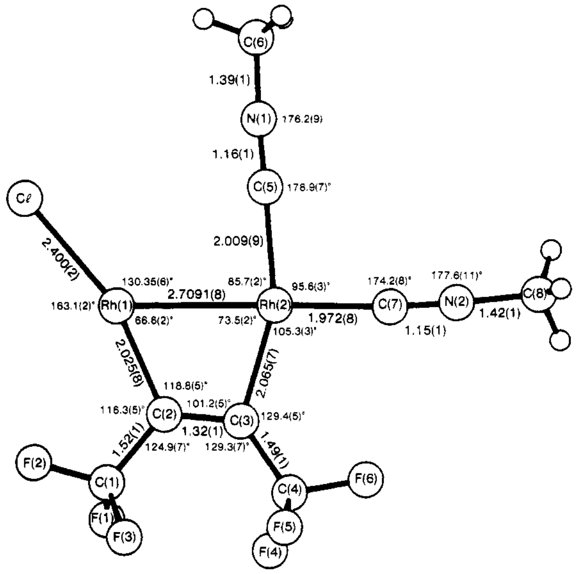

Figure 2. A view of the inner coordination sphere of $[Rh_2Cl(CNMe)_2(\mu\text{-HFB})(DPM)_2]^+$ in the approximate plane of the metals and the hexafluoro-2-butyne group. Some relevant parameters are shown.

attached carbons), and a representation of the inner coordination sphere in the plane of the acetylene and the rhodium atoms together with some relevant bond distances and angles is given in Figure 2. More complete listings of interatomic distances and angles may be found in Tables VI and VII, respectively.

The tetrafluoroborate anion has a near-tetrahedral geometry but is significantly distorted from the idealized case; the B–F distances range from 1.25 (2)–1.35 (2) Å and the F–B–F angles range from 96 (2)° to 125 (2)°. As noted earlier, this group is probably disordered, so the geometry, although not completely satisfactory, is not unexpected and compares adequately with geometries observed for other disordered BF_4^- anions.[22]

The cation has an inner-core geometry similar to that observed for many other DPM-bridged binuclear complexes, having two rhodium atoms bridged by two mutually trans DPM ligands. In the equatorial plane (perpendicular to the Rh–P vectors) the metals are bridged by a hexafluoro-2-butyne molecule coordinated as a cis-dimetalated olefin, while Rh(1) has a terminal chloro ligand and Rh(2) has two terminal, linear methyl isocyanide ligands. The metals are also connected by a metal–metal bond.

Table IV. Positional and Equivalent Isotropic Thermal Parameters for the Nongroup Atoms of $[Rh_2Cl(CNMe)_2(\mu\text{-HFB})(DPM)_2][BF_4]$

atom	x^a	y	z	B_{equiv}, Å^2
Rh(1)	0.10197 (3)	0.17210 (3)	−0.06797 (3)	2.88
Rh(2)	0.20603 (3)	0.27677 (3)	−0.09089 (3)	2.84
Cl	0.1238 (2)	0.0821 (1)	0.0185 (1)	4.83
P(1)	0.1497 (1)	0.0920 (1)	−0.1356 (1)	3.13
P(2)	0.2573 (1)	0.2068 (1)	−0.1690 (1)	3.16
P(3)	0.0391 (1)	0.2430 (1)	−0.0023 (1)	3.23
P(4)	0.1448 (1)	0.3631 (1)	−0.0314 (1)	3.31
F(1)	−0.0944 (3)	0.2641 (3)	−0.1773 (4)	6.78
F(2)	−0.0670 (3)	0.1538 (3)	−0.1691 (3)	5.33
F(3)	−0.0487 (4)	0.2108 (4)	−0.2542 (3)	7.12
F(4)	−0.0005 (3)	0.3647 (3)	−0.2371 (3)	5.73
F(5)	0.0739 (3)	0.2991 (3)	−0.2849 (3)	5.34
F(6)	0.1310 (3)	0.3869 (3)	−0.2226 (3)	5.57
F(7)	0.549 (1)	0.2828 (8)	0.0537 (9)	22.5
F(8)	0.4675 (6)	0.358 (1)	0.0188 (6)	19.3
F(9)	0.5615 (8)	0.3731 (7)	0.1178 (6)	15.8
F(10)	0.5984 (9)	0.369 (1)	0.0267 (9)	22.4
N(1)	0.3362 (4)	0.2161 (4)	0.0390 (4)	4.32
N(2)	0.3228 (5)	0.4022 (4)	−0.1113 (4)	4.93
C(1)	−0.0393 (5)	0.2143 (5)	−0.1877 (4)	4.08
C(2)	0.0506 (4)	0.2330 (4)	−0.1498 (4)	3.14
C(3)	0.0960 (4)	0.2853 (4)	−0.1664 (4)	3.10
C(4)	0.0756 (5)	0.3336 (5)	−0.2260 (5)	4.16
C(5)	0.2888 (5)	0.2390 (4)	−0.0085 (4)	3.39
C(6)	0.3960 (8)	0.1927 (7)	0.0957 (6)	7.25
C(7)	0.2785 (5)	0.3556 (5)	−0.1075 (4)	3.66
C(8)	0.3805 (8)	0.4580 (7)	−0.1145 (8)	8.70
C(9)	0.1829 (4)	0.1359 (4)	−0.2040 (4)	3.11
C(10)	0.0393 (4)	0.3374 (4)	−0.0262 (4)	3.37
B	0.540 (1)	0.354 (1)	0.056 (1)	8.65

[a] Estimated standard deviations in the last significant figure(s) are given in parentheses in this and all subsequent tables.

Each end of the $[Rh_2Cl(CNMe)_2(\mu\text{-HFB})(DPM)_2]^+$ cation rather closely resembles one of two structurally characterized complexes; on the Rh(1) side, the geometry is reminiscent of that of the precursor 1[1] whereas the geometry about Rh(2) closely approximates that observed for $[Rh_2(CN\text{-}t\text{-}Bu)_4(\mu\text{-HFB})(DPM)_2]^{2+}$, which has recently been characterized by Mague et al.[23,24] The slight differences between the coordination geometries of each metal in compound **12b** and those in the respective, related complexes seem to result from the different steric demands of the ligands involved. Therefore, in compound **12b** the chloro ligand is much closer to being trans to the acetylene moiety than in 1; this may be responsible for the longer Rh–Cl bond in the present compound (2.400 (2) Å vs. 2.377 (2) and 2.384 (2) Å in compound 1) since a σ-alkenyl group (a metalated olefin in our terminology) has a large trans influence.[25] In $[Rh_2Cl_2(\mu\text{-CO})(\mu\text{-DMA})(DPM)_2]$, the CO adduct of compound 3, the chloro ligands are similarly situated with respect to the acetylene group and the Rh–Cl distances are again long.[4] It seems that the difference in position between the Cl ligand in the present compound and those in compound 1 can be rationalized on the basis of the nonbonded contacts with the phenyl hydrogens H(12) and H(22) (see Table VI); moving the Cl atom toward the position it formerly occupied in 1 would bring about a more unfavorable contact with H(22).

The coordination about Rh(2) differs most significantly from that observed for the metals in $[Rh_2(CN\text{-}t\text{-}Bu)_4(\mu\text{-HFB})(DPM)_2]^{2+}$ owing mainly to the relative positions of the isocyanide groups; either these groups are trans to the acetylene group or to the Rh–Rh bond. In compound **12b** one CNMe group is essentially

---

[22] (a) Krogsrud, S.; Toniolo, L.; Croatto, U.; Ibers, J. A. *J. Am. Chem. Soc.* **1977**, *99*, 5277. (b) Loghry, R. A.; Simonsen, S. H. *Inorg. Chem.* **1978**, *17*, 1986. (c) Cowie, M.; Dwight, S. K. *Inorg. Chem.* **1979**, *18*, 2700. (d) Cowie, M.; Gauthier, M. D. *Inorg. Chem.* **1980**, *19*, 3142.

[23] Mague, J. T.; DeVries, S. H. *Inorg. Chem.* **1982**, *21*, 1632.

[24] Mague, J. T. *Inorg. Chem.* **1983**, *22*, 1158.

[25] Cowie, M.; Ibers, J. A. *Inorg. Chem.* **1976**, *15*, 552 and references therein.

Table V. Derived Parameters for the Rigid-Group Atoms of $[Rh_2Cl(MeNC)_2(\mu\text{-HFB})(DPM)_2][BF_4]$

atom	*x*	*y*	*z*	*B*, Å^2	atom	*x*	*y*	*z*	*B*, Å^2
C(11)	0.2388 (3)	0.0323 (3)	−0.1015 (3)	3.6 (1)	C(51)	0.079 (1)	0.2443 (4)	0.0895 (7)	3.6 (2)
C(12)	0.2941 (4)	0.0472 (3)	−0.0394 (4)	4.1 (2)	C(52)	0.0269 (4)	0.2664 (4)	0.1302 (6)	4.4 (2)
C(13)	0.3667 (3)	0.0061 (3)	−0.0169 (3)	5.7 (2)	C(53)	0.0590 (9)	0.2723 (4)	0.200 (1)	5.7 (2)
C(14)	0.3839 (3)	−0.0497 (3)	−0.0565 (3)	5.8 (2)	C(54)	0.143 (1)	0.2560 (4)	0.2287 (7)	6.5 (2)
C(15)	0.3286 (4)	−0.0645 (3)	−0.1187 (4)	5.3 (2)	C(55)	0.1953 (4)	0.2339 (4)	0.1881 (6)	6.0 (2)
C(16)	0.2560 (3)	−0.0235 (3)	−0.1412 (3)	4.6 (2)	C(56)	0.1632 (9)	0.2281 (4)	0.119 (1)	4.7 (2)
C(21)	0.0664 (4)	0.0307 (3)	−0.1775 (4)	3.1 (1)	C(61)	−0.0721 (3)	0.2208 (3)	−0.0155 (2)	3.8 (2)
C(22)	0.0306 (6)	−0.0126 (3)	−0.1366 (2)	3.9 (2)	C(62)	−0.0919 (3)	0.1483 (3)	−0.0151 (3)	4.7 (2)
C(23)	−0.0339 (5)	−0.0598 (3)	−0.1657 (4)	4.7 (2)	C(63)	−0.1757 (4)	0.1269 (2)	−0.0268 (4)	6.2 (2)
C(24)	−0.0626 (4)	−0.0639 (3)	−0.2357 (4)	4.5 (2)	C(64)	−0.2398 (3)	0.1778 (3)	−0.0388 (2)	7.0 (3)
C(25)	−0.0268 (6)	−0.0206 (3)	−0.2766 (2)	4.1 (2)	C(65)	−0.2200 (3)	0.2502 (3)	−0.0391 (3)	6.3 (2)
C(26)	0.0377 (5)	0.0266 (3)	−0.2475 (4)	3.8 (2)	C(66)	−0.1362 (4)	0.2717 (2)	−0.0275 (4)	4.8 (2)
C(31)	0.3618 (3)	0.1654 (3)	−0.1410 (2)	3.6 (2)	C(71)	0.202 (1)	0.3853 (4)	0.0548 (8)	3.8 (2)
C(32)	0.4242 (4)	0.2001 (3)	−0.0927 (3)	4.4 (2)	C(72)	0.1594 (7)	0.4098 (4)	0.1017 (6)	5.5 (2)
C(33)	0.5073 (4)	0.1763 (3)	−0.0793 (3)	5.6 (2)	C(73)	0.204 (1)	0.4272 (4)	0.1670 (4)	6.8 (3)
C(34)	0.5281 (3)	0.1179 (3)	−0.1143 (2)	5.9 (2)	C(74)	0.292 (1)	0.4202 (4)	0.1853 (8)	6.6 (3)
C(35)	0.4657 (4)	0.0832 (3)	−0.1626 (3)	5.7 (2)	C(75)	0.3342 (7)	0.3957 (4)	0.1384 (6)	5.8 (2)
C(36)	0.3826 (4)	0.1069 (3)	−0.1760 (3)	4.2 (2)	C(76)	0.289 (1)	0.3783 (4)	0.0732 (4)	4.5 (2)
C(41)	0.2761 (7)	0.2510 (3)	−0.2443 (4)	3.2 (1)	C(81)	0.1304 (4)	0.4528 (3)	−0.0688 (3)	3.7 (2)
C(42)	0.2299 (3)	0.2332 (3)	−0.3091 (5)	3.9 (2)	C(82)	0.0563 (4)	0.4721 (3)	−0.1155 (3)	4.7 (2)
C(43)	0.2534 (7)	0.2604 (3)	−0.3652 (2)	4.9 (2)	C(83)	0.0503 (4)	0.5386 (3)	−0.1472 (3)	6.1 (2)
C(44)	0.3231 (7)	0.3054 (3)	−0.3565 (4)	4.9 (2)	C(84)	0.1183 (4)	0.5857 (3)	−0.1322 (3)	6.2 (2)
C(45)	0.3693 (3)	0.3231 (3)	−0.2917 (5)	4.8 (2)	C(85)	0.1924 (4)	0.5663 (3)	−0.0854 (3)	6.0 (2)
C(46)	0.3458 (7)	0.2959 (3)	−0.2356 (2)	4.1 (2)	C(86)	0.1984 (4)	0.4999 (3)	−0.0538 (3)	4.9 (2)

Rigid-Group Parameters

	Xc[a]	*Yc*	*Zc*	δ[b]	ϵ	η
ring 1	0.3113 (3)	−0.0087 (2)	−0.0790 (2)	−0.682 (4)	2.435 (5)	0.788 (4)
ring 2	0.0019 (2)	−0.0166 (2)	−0.2066 (2)	0.790 (3)	1.850 (5)	2.017 (4)
ring 3	0.4450 (3)	0.1416 (2)	−0.1277 (2)	−0.662 (4)	2.925 (5)	0.416 (4)
ring 4	0.2996 (2)	0.2782 (2)	−0.3004 (2)	0.918 (4)	1.817 (6)	3.786 (5)
ring 5	0.1111 (3)	0.2502 (2)	0.1591 (2)	−1.258 (4)	2.19 (1)	6.03 (1)
ring 6	−0.1560 (3)	0.1993 (2)	−0.0271 (2)	3.091 (4)	0.061 (4)	5.990 (3)
ring 7	0.2468 (3)	0.4028 (2)	0.1201 (2)	−1.226 (4)	2.86 (1)	5.52 (1)
ring 8	0.1243 (3)	0.5192 (2)	−0.1005 (2)	0.410 (4)	2.751 (4)	4.476 (4)

[a] *Xc*, *Yc*, and *Zc* are the fractional coordinates of the centroid of the rigid group. [b] The rigid group orientation angles δ, ϵ, and η (radians) are the angles by which the rigid body is rotated with respect to a set of axes *x*, *y*, and *z*. The origin is the center of the ring: *x* is parallel to *a**. *z* is parallel to *c* and *y* is parallel to the line defined by the intersection of the plane containing *a** and *b** with the plane containing *b* and *c*.

trans to the Rh–Rh bond while the other is almost at right angles to it but bent toward Rh(1), away from the position which is trans to the acetylene group (see Figure 2). In Mague's species,[24] on the other hand, the two *tert*-butyl isocyanides that are mutually cis on adjacent metals are bent away from each other and are trans to the two Rh–acetylene linkages, while the other two are bent significantly off the Rh–Rh axis. These differences in isocyanide positions are probably a consequence of the significant differences in the bulk of the isocyanide groups and of the much less crowded environment around Rh(1) in the present compound (having one Cl ligand instead of two CN-*t*-Bu groups). The isocyanides tend to assume positions that minimize contacts with each other and with the DPM phenyl groups. Thus, in Figure 1 we see that these phenyl groups tend to be staggered with respect to the equatorial ligands.

The geometries of the isocyanide ligands in **12b** are normal for terminally bonded, linear isocyanide groups and agree well with each other and with other reported parameters.[26-28] Although the two metal–isocyanide distances differ slightly (1.972 (8), 2.009 (9) Å), the difference is in the direction expected, with the longer distance being the one trans to a group of high trans influence (the metalated olefin). These distances are significantly shorter than those observed for the *tert*-butyl isocyanide groups in Mague's compound.[24] However, it is likely that the rather long distances in the latter species result from the severe crowding in this molecule.

The overall geometry of the bridging acetylene ligand is not atypical for such a group when bonding as a cis-demetalated olefin, having angles about the metalated carbons that are reminiscent of sp^2 hybridization and an acetylenic C–C bond that has lengthened to 1.32 (1) Å, close to that of a normal olefin.[29] However, this acetylene group is coordinated in an unsymmetrical manner, appearing to be more tightly bound to Rh(1), as evidenced by the shorter rhodium–carbon distance (2.025 (8) vs. 2.065 (7) Å). In addition, it is displaced in the equatorial plane such that C(2) is only 2.660 (7) Å from Rh(2), whereas the corresponding Rh(1)–C(3) distance is 2.902 (7) Å. Although this contact with Rh(2) is well beyond that of a normal covalent bond, it may suggest some interaction of Rh(2) with the C(2)–C(3) π-bond. In the acetylide-bridged A-frame, $[Rh_2(CO)_2(\mu\text{-CC-}t\text{-Bu})(DPM)_2][ClO_4]$, the acetylide moiety is coordinated to one metal in a side-on manner and the two Rh–C distances involved are 2.209 (6) and 2.616 (6) Å,[30] suggesting that the above contact in the present complex is not unreasonable for some π-interaction. Such an interaction is also consistent with the drop in the infrared stretch associated with the acetylene moiety from 1642 cm^{-1} in 1 to 1590 cm^{-1} in **12b**. This asymmetry could, however, be steric in origin since it is consistent with the end of the acetylene ligand, which is adjacent to the crowded isocyanide end of the complex, being forced away from Rh(2) (see Figure 2). The nonbonded contact between C(7) and F(6) of 2.98 (1) Å is consistent with these steric arguments, although it seems as through any unfavorable steric interactions could have been relieved by twisting the acetylene moiety out of the plane containing the rhodium atoms, the chloro ligand, and the isocyanide ligands as was observed in the *tert*-butyl isocyanide complex.[24] As it is, the acetylene moiety

---

(26) Olmstead, M. M.; Hope, H.; Benner, L. S.; Balch, A. L. *J. Am. Chem. Soc.* **1977**, *99*, 5502.

(27) Goldberg, S. Z.; Eisenberg, R. *Inorg. Chem.* **1976**, *15*, 58.

(28) Goldberg, S. Z.; Eisenberg, R. *Inorg. Chem.* **1976**, *15*, 535.

(29) MacGillavry, C. H.; Rieck, G. D. "International Tables for X-ray Crystallography"; Kynoch Press: Birmingham, England, 1968; Vol. III, Table 4.2.2.

(30) Cowie, M.; Loeb, S. J., submitted for publication.

Table VI. Selected Distances (Å) in $[Rh_2Cl(MeNC)_2(\mu\text{-}HFB)(DPM)_2][BF_4]$

Bonding Distances

Rh(1)-Rh(2)	2.7091 (8)	C(4)-F(4)	1.342 (9)
Rh(1)-Cl	2.400 (2)	C(4)-F(5)	1.360 (10)
Rh(1)-P(1)	2.301 (2)	C(4)-F(6)	1.338 (9)
Rh(1)-P(3)	2.302 (2)	P(1)-C(9)	1.815 (8)
Rh(2)-P(2)	2.371 (2)	P(2)-C(9)	1.821 (7)
Rh(2)-P(4)	2.384 (2)	P(3)-C(10)	1.831 (8)
Rh(1)-C(2)	2.025 (8)	P(4)-C(10)	1.821 (7)
Rh(2)-C(3)	2.065 (7)	P(1)-C(11)	1.831 (4)
Rh(2)-C(5)	2.009 (9)	P(1)-C(21)	1.823 (4)
Rh(2)-C(7)	1.972 (8)	P(2)-C(31)	1.835 (4)
C(2)-C(3)	1.322 (10)	P(2)-C(41)	1.838 (4)
C(1)-C(2)	1.523 (10)	P(3)-C(51)	1.827 (5)
C(3)-C(4)	1.486 (11)	P(3)-C(61)	1.822 (5)
C(5)-N(1)	1.162 (10)	P(4)-C(71)	1.826 (5)
C(7)-N(2)	1.148 (10)	P(4)-C(81)	1.833 (5)
C(6)-N(1)	1.389 (12)	B-F(7)	1.35 (2)
C(8)-N(2)	1.420 (12)	B-F(8)	1.25 (2)
C(1)-F(1)	1.349 (10)	B-F(9)	1.27 (2)
C(1)-F(2)	1.309 (9)	B-F(10)	1.27 (2)
C(1)-F(3)	1.329 (10)		

Nonbonded Distances

P(1)-P(2)	2.961 (3)	Cl-H(12)	2.82
P(3)-P(4)	2.982 (3)	C(5)-H(76)	2.50
Rh(1)-C(3)	2.902 (7)	C(5)-H(32)	2.58
Rh(2)-C(2)	2.660 (7)	H(1C10)-H(72)	2.05
Rh(1)-F(2)	3.033 (5)	H(2C9)-H(36)	2.10
Rh(2)-F(6)	3.369 (5)	R(1)^a-H(73)^b	2.59
F(6)-C(7)	2.981 (10)	R(2)^a-H(34)^c	2.61
Cl-H(22)	2.81	R(3)^a-H(3C6)	2.61

[a] R(1), R(2), and R(3) are three of the five most intense residual Fourier peaks. [b] H(73) of the molecule at $(1 - x, -y, -z)$. [c] H(34) of the molecule at $(^1/_2 - x, y - ^1/_2, ^1/_2 - z)$.

is twisted from the above plane by only 0.9 (6)°. Whatever the reason for the observed asymmetry in acetylene bonding, we would expect to observe less activation at the acetylenic carbon which is less tightly bound to the metal (C(3)) and therefore less bending back of the CF_3 group and a shorter C–CF_3 bond (the covalent radius for an sp carbon is less than that of an sp^2 carbon). Both of these effects are observed, although the difference in the C–CF_3 bonds is not statistically significant and may therefore be fortuitous. However, the difference in the C(2)–C(3)–C(4) and the C(3)–C(2)–C(1) angles is significant, especially since it is the opposite to what would be expected based on steric interaction between this CF_3 group and the neighboring isocyanide ligand. In another complex recently characterized by Mague, $[Rh_2(O_2CMe)(P(OMe)_3)(\mu\text{-}CO)(\mu\text{-}MDA)(DPM)_2]$ $PF_6{\cdot}Me_2CO$,[31] the difference in Rh–$C_{acetylene}$ distances is even more pronounced (1.985 (12) and 2.053 (12) Å) than in our compound, but here there is no significant difference in the angles about the acetylenic carbons. It may also be that in the present determination the difference in the bendback angles of the CF_3 groups is also steric in origin since F(2) is involved in a rather close contact with Rh(1) (3.033 (5) Å) which could force this CF_3 group away from Rh(1) resulting in a more acute C(1)–C(2)–C(3) angle.

The Rh(1)–Rh(2) distance (2.7091 (8) Å), although typical for a Rh–Rh single bond, is one of the shortest yet observed in DPM-bridged dirhodium systems. Since each end in the present compound resembles either $[Rh_2Cl_2(\mu\text{-}CF_3C_2CF_3)(DPM)_2]$ or $[Rh_2(CN\text{-}t\text{-}Bu)_4(\mu\text{-}CF_3C_2CF_3)(DPM)_2]^{2+}$, it might be expected that its Rh–Rh distance would be intermediate between those in the above complexes. In fact, it is less than either of these. However, it should be noted that the Rh–Rh distance in the tetrakis(*tert*-butyl isocyanide) dication[24] (2.9653 (6) Å) is anomalously long, most probably due to severe crowding about both metal centers. The $Rh_2(DPM)_2$ framework in **12b** is essentially as expected, with some minor distortions. Both diphosphine ligands are bent toward the bridging acetylene group, reflecting the nonbonded interactions of the phenyl groups with the chloro ligand and the isocyanide groups; since the bridging methylene groups of the DPM ligands are bent toward the acetylene ligand, phenyl groups 1, 3, 5, and 7 are thrust toward the isocyanide ($C(5)N(1)C(6)H_3$) and Cl ligands so interactions of these groups seem to dictate the phosphine geometries. All Rh–P distances (2.301 (2)–2.384 (2) Å) are within the range normally observed for such DPM-bridged, dirhodium compounds,[32] although those on Rh(1) are significantly shorter than those on Rh(2). It seems that the longer distances reflect the more crowded environment about Rh(2). In two other A-frame-like compounds, $[Rh_2Cl_3(\mu\text{-}H)(\mu\text{-}CO)(DPM)_2]$[6] and $[Rh_2Cl_2(CO)(SCNMe_2)(DPM)_2][BF_4]$,[33] similar variations in the Rh–P distances were also observed, with the longer distances being associated with the more crowded rhodium centers. All other parameters within the phosphine groups in the present compound are normal.

Discussion of Results

(a) Reactions with CO and SO_2. At the time that this work was undertaken, the only confirmed examples of CO insertion into metal–metal single bonds had been reported for $[M_2X_2(Ph_2YCH_2YPh_2)_2]$ (M = Pd, Pt; Y = P, As),[34,35] and even now examples of such reactions are rare.[34-36] Although we had not previously observed such insertions in related dirhodium, DPM-bridged complexes, the reaction of $[Rh_2X_2(\mu\text{-}CO)(DPM)_2]$ with acetylenes to give $[Rh_2X_2(\mu\text{-}CO)(\mu\text{-}acetylene)(DPM)_2]$ suggested to us that CO insertion into the Rh–Rh bond of the acetylene-bridged species **1**, to give a product analogous to the above carbonyl- and acetylene-bridged complexes, might be possible.

Examples of SO_2 insertions into metal–metal bonds, on the other hand, have been known for some time,[37,38] although such insertions into the Rh–Rh bonds of DPM-bridged A-frames had apparently not been observed and certainly no evidence of direction insertion had been observed by us.[5] Again, it seemed that compound **1**, and the related species **2** and **3**, should be capable of undergoing SO_2 insertion into the Rh–Rh bonds.

The initial reactions of compounds **1**, **2**, and **3** with CO and SO_2 do in fact yield species that seem to have resulted from the insertion of these small molecules into the metal–metal bonds as diagrammed in eq 1. For the products of CO insertion (**4**, **5**, and **6**) the $^{31}P\{^1H\}$ NMR spectra are all rather similar and are as expected for symmetrical products.[14] Furthermore, the infrared spectra show the stretch of the bridging carbonyl ligand at ca. 1700 cm^{-1} for each product. Although this frequency is rather low, it is typical for carbonyl groups which bridge two metals not accompanied by a metal-metal bond.[4,34,35] Of course, the above spectral parameters are exactly those observed in the reactions of $[Rh_2X_2(\mu\text{-}CO)(DPM)_2]$ with the appro-

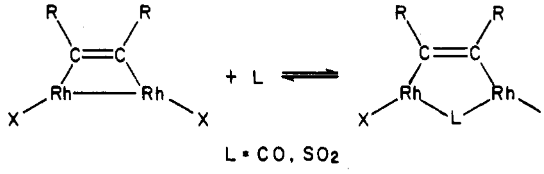

(1)

---

[31] Mague, J. T. *Inorg. Chem.* **1982**, *22*, 45.

[32] Puddephatt, R. J. *Chem. Soc. Rev.* **1983**, *12*, 99.

[33] Gibson, J. A. E.; Cowie, M. *Organometallics* **1984**, *3*, 722.

[34] (a) Colton, R.; McCormick, M. J.; Pannan, C. D. *J. Chem. Soc., Chem. Commun.* 1977, 823. (b) Colton, R.; McCormick, M. J.; Pannan, C. D. *Aust. J. Chem.* **1978**, *31*, 1425.

[35] Brown, M. P., Keith, A. N.; Manojlovic-Muir, Lu.; Muir, K. W.; Puddephatt, R. J.; Seddon, K. R. *Inorg. Chim. Acta* **1979**, *34*, L223.

[36] Pringle, P. G.; Shaw, B. L. *J. Chem. Soc., Dalton Trans.* **1983**, 889.

[37] Ruff, J. K. *Inorg. Chem.* **1967**, *6*, 2080.

[38] (a) Benner, L. S.; Olmstead, M. M.; Hope, H.; Balch, A. L. *J. Organomet. Chem.* **1978**, *153*, C31. (b) Balch, A. L.; Benner, L. S.; Olmstead, M. M. *Inorg. Chem.* **1979**, *18*, 2996.

Table VII. Selected Angles (deg) in $[Rh_2Cl(MeNC)_2(\mu\text{-}HFB)(DPM)_2][BF_4]$

Bond Angles

P(1)-Rh(1)-Rh(2)	92.56 (5)	F(2)-C(1)-C(2)	114.2 (7)	C(31)-P(2)-C(41)	96.5 (3)
P(3)-Rh(1)-Rh(2)	94.37 (5)	F(3)-C(1)-C(2)	112.5 (7)	C(10)-P(3)-C(51)	103.7 (3)
P(2)-Rh(2)-Rh(1)	93.49 (5)	F(4)-C(4)-C(3)	114.4 (7)	C(10)-P(3)-C(61)	104.4 (3)
P(4)-Rh(2)-Rh(1)	92.22 (5)	F(5)-C(4)-C(3)	112.8 (7)	C(51)-P(3)-C(61)	104.2 (3)
P(1)-Rh(1)-P(3)	172.61 (7)	F(6)-C(4)-C(3)	113.6 (7)	C(10)-P(4)-C(71)	105.6 (3)
P(2)-Rh(2)-P(4)	168.34 (7)	F(1)-C(1)-F(2)	104.8 (7)	C(10)-P(4)-C(81)	103.8 (3)
Cl-Rh(1)-Rh(2)	130.35 (6)	F(1)-C(1)-F(3)	106.4 (7)	C(71)-P(4)-C(81)	100.1 (3)
Cl-Rh(1)-P(1)	88.57 (7)	F(2)-C(1)-F(3)	107.1 (7)	P(1)-C(9)-P(2)	109.1 (4)
Cl-Rh(1)-P(3)	88.91 (8)	F(4)-C(4)-F(5)	104.0 (7)	P(3)-C(10)-P(4)	109.5 (4)
Cl-Rh(1)-C(2)	163.1 (2)	F(4)-C(4)-F(6)	105.9 (7)	P(1)-C(11)-C(12)	120.2 (3)
P(1)-Rh(1)-C(2)	90.2 (2)	F(5)-C(4)-F(6)	105.3 (7)	P(1)-C(11)-C(16)	119.5 (3)
P(3)-Rh(1)-C(2)	90.2 (2)	Rh(2)-C(5)-N(1)	178.9 (7)	P(1)-C(21)-C(22)	117.4 (3)
P(2)-Rh(2)-C(3)	85.9 (2)	Rh(2)-C(7)-N(2)	174.2 (8)	P(1)-C(21)-C(26)	122.6 (3)
P(4)-Rh(2)-C(3)	86.0 (2)	C(5)-N(1)-C(6)	176.2 (9)	P(2)-C(31)-C(32)	119.2 (3)
C(5)-Rh(2)-C(3)	159.1 (3)	C(7)-N(2)-C(8)	177.6 (1)	P(2)-C(31)-C(36)	119.9 (3)
C(7)-Rh(2)-C(3)	105.3 (3)	Rh(1)-P(1)-C(9)	112.2 (2)	P(2)-C(41)-C(42)	121.7 (3)
C(2)-Rh(1)-Rh(2)	66.6 (2)	Rh(1)-P(1)-C(11)	121.6 (2)	P(2)-C(41)-C(46)	117.7 (3)
C(3)-Rh(2)-Rh(1)	73.5 (2)	Rh(1)-P(1)-C(21)	111.5 (2)	P(3)-C(51)-C(52)	120.0 (3)
C(5)-Rh(2)-Rh(1)	85.7 (2)	Rh(2)-P(2)-C(9)	110.5 (2)	P(3)-C(51)-C(56)	119.8 (3)
C(7)-Rh(2)-Rh(1)	177.9 (2)	Rh(2)-P(2)-C(31)	118.8 (2)	P(3)-C(61)-C(62)	116.5 (3)
C(5)-Rh(2)-C(7)	95.6 (3)	Rh(2)-P(2)-C(41)	118.4 (2)	P(3)-C(61)-C(66)	123.5 (3)
P(2)-Rh(2)-C(5)	95.3 (2)	Rh(1)-P(3)-C(10)	111.6 (3)	P(4)-C(71)-C(72)	121.1 (3)
P(4)-Rh(2)-C(5)	95.3 (2)	Rh(1)-P(3)-C(51)	120.6 (2)	P(4)-C(71)-C(76)	118.9 (3)
P(2)-Rh(2)-C(7)	88.2 (2)	Rh(1)-P(3)-C(61)	110.9 (2)	P(4)-C(81)-C(82)	121.5 (3)
P(4)-Rh(2)-C(7)	85.9 (2)	Rh(2)-P(4)-C(10)	112.1 (3)	P(4)-C(81)-C(86)	118.2 (3)
Rh(1)-C(2)-C(3)	118.8 (5)	Rh(2)-P(4)-C(71)	117.8 (2)	F(7)-B-F(8)	97 (2)
Rh(2)-C(3)-C(2)	101.2 (5)	Rh(2)-P(4)-C(81)	115.7 (2)	F(7)-B-F(9)	108 (2)
Rh(1)-C(2)-C(1)	116.3 (5)	C(9)-P(1)-C(11)	101.9 (3)	F(7)-B-F(10)	96 (2)
Rh(2)-C(3)-C(4)	129.4 (5)	C(9)-P(1)-C(21)	104.8 (3)	F(8)-B-F(9)	125 (2)
C(1)-C(2)-C(3)	124.9 (7)	C(11)-P(1)-C(21)	103.2 (3)	F(8)-B-F(10)	114 (2)
C(2)-C(3)-C(4)	129.3 (7)	C(9)-P(2)-C(31)	107.3 (3)	F(9)-B-F(10)	111 (1)
F(1)-C(1)-C(2)	111.1 (7)	C(9)-P(2)-C(41)	103.4 (3)		

Torsion Angles

P(1)-Rh(1)-Rh(2)-P(2)	3.94 (7)	C(51)-P(3)-P(4)-C(71)	−0.4 (3)	C(21)-P(1)-Rh(1)-C(2)	−81.0 (3)
P(3)-Rh(1)-Rh(2)-P(4)	−3.65 (7)	C(61)-P(3)-P(4)-C(81)	2.9 (5)	C(51)-P(3)-Rh(1)-C(2)	−159.8 (3)
P(1)-Rh(1)-Rh(2)-P(4)	173.77 (7)	C(11)-P(1)-Rh(1)-Cl	−39.9 (2)	C(61)-P(3)-Rh(1)-C(2)	78.2 (3)
P(3)-Rh(1)-Rh(2)-P(2)	−173.47 (7)	C(21)-P(1)-Rh(1)-Cl	82.1 (2)	C(31)-P(2)-Rh(2)-C(3)	−175.7 (3)
C(9)-P(1)-P(3)-C(10)	−1.7 (4)	C(51)-P(3)-Rh(1)-Cl	37.1 (2)	C(41)-P(2)-Rh(2)-C(3)	67.9 (3)
C(9)-P(2)-P(4)-C(10)	0.3 (4)	C(61)-P(3)-Rh(1)-Cl	−84.9 (2)	C(71)-P(4)-Rh(2)-C(3)	174.5 (3)
C(11)-P(1)-P(3)-C(51)	−2.8 (3)	C(31)-P(2)-Rh(2)-C(5)	−16.6 (3)	C(81)-P(4)-Rh(2)-C(3)	−67.2 (3)
C(21)-P(1)-P(3)-C(61)	−2.7 (3)	C(41)-P(2)-Rh(2)-C(5)	−133.0 (3)	C(9)-P(1)-Rh(1)-C(2)	36.1 (3)
C(31)-P(2)-P(4)-C(71)	−1.3 (3)	C(71)-P(4)-Rh(2)-C(5)	15.4 (3)	C(10)-P(3)-Rh(1)-C(2)	−37.7 (3)
C(41)-P(2)-P(4)-C(81)	0.6 (3)	C(81)-P(4)-Rh(2)-C(5)	133.8 (3)	C(9)-P(2)-Rh(2)-C(3)	−51.1 (3)
C(1)-C(2)-C(3)-C(4)	5.1 (13)	C(31)-P(2)-Rh(2)-C(7)	78.8 (3)	C(10)-P(4)-Rh(2)-C(3)	51.6 (3)
Rh(1)-C(2)-C(3)-Rh(2)	−0.9 (6)	C(41)-P(2)-Rh(2)-C(7)	−37.6 (3)	Cl-Rh(1)-C(2)-C(1)	2.6 (12)
Cl-Rh(1)-Rh(2)-C(5)	−0.8 (2)	C(71)-P(4)-Rh(2)-C(7)	−79.8 (3)	C(5)-Rh(2)-C(3)-C(4)	−174.7 (8)
C(11)-P(1)-P(2)-C(31)	0.4 (3)	C(81)-P(4)-Rh(2)-C(7)	38.5 (3)	C(7)-Rh(2)-C(3)-C(4)	6.4 (8)
C(21)-P(1)-P(2)-C(41)	−2.4 (4)	C(11)-P(1)-Rh(1)-C(2)	156.9 (3)		

priate acetylene molecule[4] and confirm that identical products are obtained by either route. The X-ray structure determination of one product, $[Rh_2Cl_2(\mu\text{-}CO)(\mu\text{-}DMA)(DPM)_2]$, has unambiguously confirmed the above formulations and shows a carbonyl geometry which corresponds to sp^2 hybridization, in agreement with the low carbonyl stretching frequency.[4]

The products obtained in the reactions of compounds **1**, **2**, and **3** with SO_2 are analogous to the above carbonyl adducts and are therefore formulated as $[Rh_2X_2(\mu\text{-}SO_2)(\mu\text{-}RC_2R)(DPM)_2]$ (R = CF_3, X = Cl (**7**), I (**8**); R = CO_2Me, X = Cl (**9**)) in which the bridging SO_2 and acetylene groups are not accompanied by a Rh–Rh bond. Although elemental analyses of pure samples cannot be obtained owing to the reversibility of the reactions (vide infra), the spectral parameters clearly support the above formulation. The S–O stretches in the infrared spectra occur at ca. 1140 and 1060 cm^{-1}. The drop in the higher frequency stretch from that usually observed when the bridging SO_2 is accompanied by a metal–metal bond[39] parallels the lower carbonyl stretching frequencies observed for the carbonyl-bridged analogues **4**, **5**, and **6**. In addition, the $^{31}P\{^1H\}$ NMR spectra of the SO_2 adducts are very similar to those of the CO adducts, again showing an increase (to ca. 130 Hz) in the splitting between the two major peaks as compared to the starting materials. Although these spectral results do not rule out the possibility that these symmetrical products might contain two SO_2 ligands (especially since compounds **7** and **8** are prepared under excess SO_2), the reaction of **3** with 1 equiv of SO_2 to yield only **9** excludes the possibility of major species containing more than one SO_2 group. It is of interest to note that although compounds **4**–**6** can be obtained either by reaction of compounds **1**–**3** with CO or by reaction of the corresponding carbonyl complex $[Rh_2X_2(\mu\text{-}CO)(DPM)_2]$ with the appropriate acetylene, the SO_2 adducts **7**–**9** can only be prepared by reaction of **1**–**3** with SO_2. Attempts to prepare these SO_2-bridged products by reacting $[Rh_2X_2(\mu\text{-}SO_2)(DPM)_2]$[5b] with acetylenes failed.

The reactions of CO and SO_2 with compounds **1**–**3** are all reversible, although a significant range in ligand labilities is observed, as outlined in the Experimental Sec-

---

[39] Kubas, G. J. *Inorg. Chem.* **1979**, *18*, 182.

tion. Whereas refluxing is required to remove the carbonyl groups in compounds **4**–**6**, the labile SO_2 ligands in compounds **7**–**9** can be readily removed by flushing the solutions with N_2. The SO_2 adducts of the HFB-bridged complexes are particularly labile and attempts to isolate these species yield large amounts of starting material, particularly in the case of compound **7** where mostly starting material is obtained. The small concentrations of **7** obtained and the presence of strong C–F stretches as well as bands due to DPM make location of the S–O stretches in this compound difficult. However, comparisons with spectra of the pure starting material and with those of **8** and **9** do serve to identify the weak bands. The SO_2 group in compound **9** is much less labile than in the other SO_2 adducts, although it too is lost to some degree upon recrystallization.

In all cases the acetylene groups are more tightly bound than either the carbonyl or sulfur dioxide ligands; only in the experiment in which compound **6** undergoes prolonged reflux in benzene is any acetylene loss observed.

It seems, from this study, that the iodo complexes bind CO and SO_2 more strongly than do the chloro analogues and that the DMA complexes bind these molecules more strongly than the HFB species. The first observation is consistent with the better π-donor capability of the iodo ligand compared to Cl, which results in additional electron density at the metals that can be used in π-back-bonding with the CO or SO_2 ligands causing them to be bound more strongly. The second observation suggests that HFB is a more effective electron-withdrawing group than DMA leaving less electron density on the metals for π-back-donation to CO or SO_2, thereby labilizing these groups. This is consistent with the known substituent σ-parameters for CF_3 and CO_2Me moieties,[40] which indicate that the trifluoromethyl groups on HFB have a higher group electronegativity than the methyl carboxylate groups on DMA.

Although the reactions of CO and SO_2 with compounds **1**–**3** can be most readily visualized as occurring directly at the metal–metal bond, molecular orbital calculations by Hoffmann and co-workers[41] suggest that such attack is actually symmetry forbidden and that some unsymmetrical intermediate is initially involved. Although no such intermediate was ever observed in our reactions, one cannot be ruled out. Certainly, one possible intermediate, diagrammed in eq 2, would be expected to yield the observed products (L = CO, SO_2) with great facility. Support for such a short-lived, unsymmetrical intermediate has actually been obtained for the reactions of **1**–**3** with isocyanide molecules (vide infra).

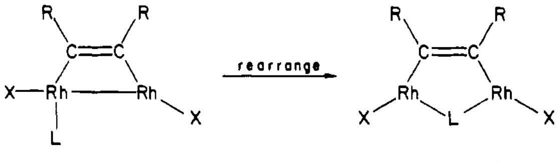

(2)

(b) Reactions with CNMe. Isocyanides, CNR, are quasi-isoelectronic with CO and might therefore be expected to behave similarly. Consequently they can function as simple π-acid ligands or they can undergo insertion reactions with metal–metal and metal–carbon bonds,[42,43] much as is observed for CO and SO_2. However, isocyanides are stronger σ-donor and poorer π-acceptor ligands than CO as exemplified by the change in infrared stretching frequencies associated with these groups upon coordination to metals,[43] whereas ν(CO) invariably decreases upon coordination to metals that are capable of π-back-donation, ν(CN) for coordinated isocyanides are often higher than those of the free molecule. More effective σ-donation from an orbital that is C–N antibonding and less effective back-donation from the metal into the C–N π^* orbitals account for the observed increase in ν(CN). This greater σ-basicity of isocyanides can lead to reactivity that differs from that normally found for CO. For example, the reaction of methyl isocyanide with $[Pd_2Cl_2(DPM)_2]$[26] initially gives the product of insertion into the Pd–Pd bond, as is observed for CO and SO_2; however, this product then reacts further with CNMe via stepwise exchange of Cl^- by CNMe to ultimately give $[Pd_2(CNMe)_2(\mu\text{-}CNMe)(DPM)_2]^{2+}$, the carbonyl analogue of which has apparently not been observed.

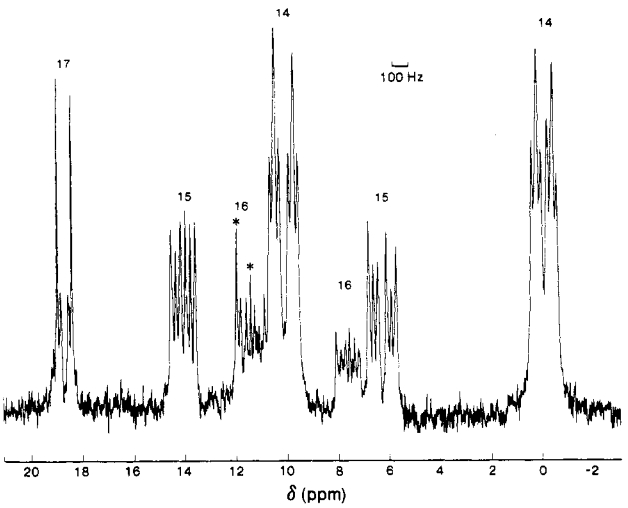

Figure 3. The $^{31}P\{^1H\}$ NMR spectrum, at 161.92 MHz, after the addition of approximately 1.3 equiv of CNMe to $[Rh_2I_2(\mu\text{-}HFB)(DPM)_2]$. The peaks marked with as asterisk are due to compound **13c** superimposed on the resonance for compound **16**.

Since the $[Rh_2X_2(\mu\text{-}RC{\equiv}CR)(DPM)_2]$ complexes display Rh–Rh bond reactivities with CO and SO_2 similar to that observed with the above Pd dimer, we chose also to examine the reactivities of the acetylene-bridged dirhodium species with CNMe, anticipating that reaction at the Rh–Rh bonds would be the first step. However, this was found not to be the case.

As described in the Experimental Section, the reactions of CNMe with compounds **1**, **2**, and **3** were carried out by sequentially adding aliquots of the isocyanide to solutions of the complexes followed by monitoring using infrared and NMR spectroscopy. A brief word regarding the $^{31}P\{^1H\}$ NMR spectra is in order before discussing the isocyanide additions. Two types of peak patterns are generally obtained in these reactions, examples of which are shown in Figure 3. For the purposes of this study we conclude that a detailed analysis of the spectra offers no additional information of relevance so no analysis was carried out, although we note that similar spectra have, on other occasions, been successfully analyzed by ourselves[33] and others.[14,23] In Table II we report the separations between the peaks; these are not the true coupling constants but are given as an aid in identifying the compounds. The first type of peak pattern is that of a species having chemically equivalent Rh nuclei (and therefore four chemically equivalent P nuclei) and appears as two major peaks with additional minor peaks (see for example complex **17** in Figure 3). As usual the splitting between the two major

---

[40] Kosower, E. M. "An Introduction to Physical Organic Chemistry"; Wiley: New York, 1968; p 49.

[41] Hoffman, D. M.; Hoffmann, R.; Fisel, C. R. *J. Am. Chem. Soc.* **1982**, *104*, 3858.

[42] Treichel, P. M. *Adv. Organomet. Chem.* **1973**, *11*, 21.

[43] Malatesta, L.; Bonati, F. "Isocyanide Complexes of Metals"; Wiley: New York, 1969.

peaks is reported. The second peak type appears as two resonances, each of which appears as two sets of three-line patterns (appearing sometimes as two pseudodoublets of triplets) and is indicative of an AA′BB′XY spin system resulting from two chemically inequivalent Rh nuclei (species **14** and **15** in Figure 3). For this spectral type the chemical shift of the center of each pair of three-line patterns is given as well as the separation between the pairs of "triplets" and the splitting within these "triplets".

After the addition of 1 equiv of CNMe to compound **1** the $^{31}P\{^1H\}$ NMR spectrum reveals four approximate doublets of triplets. Homonuclear ^{31}P decoupling reveals that they are linked in pairs; therefore irradiation of one "doublet of triplets" results in collapse of another to leave a doublet. Thus two asymmetric species **10** and **11**, in the approximate molar ratios of 4:3, respectively, are present. The ^{19}F NMR spectrum at this stoichiometry shows a coupled pair of quartets (confirmed by ^{19}F decoupling) and a broad singlet, which on the basis of their relative intensities can be assigned to compounds **10** and **11**, respectively. Similarly, the corresponding ^1H NMR spectrum reveals two new singlets at 3.32 and 2.98 ppm, in a region appropriate for coordinated CNMe groups. These methyl resonances, which again integrate in the ratio 4:3, together integrate as one CNMe group. Two sets of resonances appear for the DPM methylene protons. The solution infrared spectrum reveals two terminal isocyanide stretches as 2192 and 2212 cm^{-1}, again assigned to compounds **10** and **11**, respectively, on the basis of their intensities.

On the basis of the above spectral information, three structures seem possible for these two isomers as shown in I–III (X = Cl). In view of the very low conductivity of the reaction mixture,[15] significant dissociation of Cl$^-$ is not considered likely. Furthermore, attempts to prepare the species likely to be the result of Cl$^-$ loss, $[Rh_2Cl(CNMe)(\mu\text{-}CF_3C_2CF_3)(DPM)_2]^+$, were unsuccessful; the addition of 0.5 equiv of $AgBF_4$ in THF to a solution as above led to the formation of roughly equimolar amounts of $[Rh_2Cl(CNMe)_2(\mu\text{-HFB})(DPM)_2][BF_4]$ (vide infra) and **1**, and further $AgBF_4$ addition resulted in the decomposition of compound **1** to unidentified products. Although we are unable to unambiguously establish the structures of compounds **10** and **11**, one thing is clear—the final products are very different from those obtained upon CO(**4**) or SO_2 addition (**7**). In no case do we observe evidence of a bridging isocyanide group. Both structures I and II are clearly related to that presented earlier in the paper for compound **12b** and therefore seem feasible. Structure I is particularly interesting since a rather analogous structure was proposed earlier as an alternative to direct insertion of CO and SO_2 into the Rh–Rh bonds in compounds **1**–**3**.

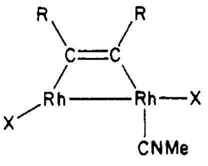

I

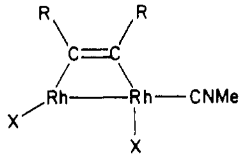

II

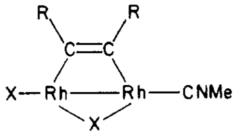

III

After the addition of 2 equiv of CNMe to a solution of **1**, one species (**12a**) predominates with a $^{31}P\{^1H\}$ NMR spectrum that is typical of an AA′BB′XY spin system arising from an unsymmetrical compound. This is confirmed by a ^{19}F NMR spectrum, which shows a pair of quartets, and by the ^1H NMR spectrum, which shows two methyl resonances. Solution infrared measurements reveal two terminal isocyanide stretches at 2192 and 2229 cm^{-1}, and conductivity measurements show that the species is a weak electrolyte.[15] Reaction of **12a** with a methanol solution of $NaBF_4$ leads to precipitation of the very insoluble species $[Rh_2Cl(CNMe)_2(\mu\text{-HFB})(DPM)_2][BF_4]$ (**12b**), whose structure was unambiguously established by X-ray techniques (vide supra). Compound **12b** has isocyanide stretches at 2216 and 2244 cm^{-1}. Owing to the very low solubility of **12b** a satisfactory $^{31}P\{^1H\}$ NMR spectrum could not obe obtained; however, its ^1H NMR spectrum shows the CNMe resonances, which are shifted somewhat from those of **12a** (see Table II). These differences, we suggest, are due to Cl$^-$ association in compound **12a**, as suggested by its low conductivity. On the basis of these data, compound **12a** is assigned the structure IV, analogous to that found for **12b**.

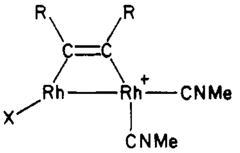

IV

The addition of CNMe to a solution of **12a** results in the formation of a new species **13a**, and after the addition of 2 equiv of CNMe, conversion to this product is complete. Compound **13a** can also be prepared by the addition of 4 equiv of CNMe to compound **1**. No other species is detected between **12a** and **13a**. The $^{31}P\{^1H\}$ NMR spectrum displays two major peaks of equal intensity, characteristic of a symmetrical species, and the ^{19}F NMR spectrum shows one singlet. The ^1H NMR spectrum reveals two resonances, each integrating as six protons, indicating that it contains four CNMe ligands grouped into two chemically equivalent pairs. Although the conductivity measurement is low for a 2:1 electrolyte, it is approximately double that found for solutions of **12a**, again suggesting association of the Cl$^-$ anions with the cation. We therefore formulate the compound as shown in V (with DPM groups omitted for clarity). This structure is similar to that reported by Mague for the CN-*t*-Bu analogue,[24] which was prepared[23] by HFB addition to $[Rh_2(CN\text{-}t\text{-}Bu)_4(DPM)_2]^{2+}$. In addition, we have prepared Mague's species, as reported above for CNMe, by the addition of 4 equiv of CN-*t*-Bu to compound **1**.[44] Clearly, the addition of 2 equiv of CNMe to **12a** brings about replacement of the remaining Cl$^-$ anion by two CNMe groups, as was observed for Cl$^-$ replacement at the first metal center. However, in this case no intermediate involving three CNMe groups analogous to the 1:1 adducts **10** and **11**, is observed. The addition of more CNMe to solutions of **13a** causes no further reaction.

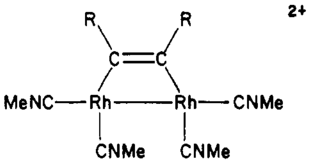

V

The stewise addition of CNMe to $[Rh_2I_2(\mu\text{-HFB})(DPM)_2]$ (**2**) has also been monitored, as described above

---

[44] Hames, B. W.; Cowie, M., unpublished results.

for compound 1, and on the whole the results are comparable, although there are some notable differences. Reaction of 2 with 1 equiv of CNMe again yields two unsymmetrical species (**14** and **15**) in approximately a 5:2 ratio. Again, which of the possible isomers (I–III) these products correspond to is not clear, although it seems, based on the ^{1}H NMR spectra, that the major isomer is analogous to the more abundant one in the reaction of compound 1 and that substitution of Cl^- by I^- favors the production of this isomer. The lower abundance of the one isomer on substituting Cl by I is consistent with the involvement of halide-bridged species such as III. Because of the lower tendency of iodine to bridge metal–metal bonds compared with chlorine, we would expect a lower abundance of the halide-bridged isomer in the iodo complex and therefore suggest that the less abundant isomer involves the halide-bridged structure III. It may be that this isomer consists not solely of compound III but of a rapidly equilibrating mix of compounds II and III, since these structures are related merely by swinging the halide ligand into or out of the bridging site. We suggest therefore that the two 1:1 adducts observed correspond to isomer I, being the more abundant one, and either isomer III or a rapidly equilibrating mix of isomers II and III as the less abundant species. Further CNMe addition results in the appearance of the unsymmetrical 2:1 adduct **16**, which is analogous to the chloro species **12a**, but also produces a symmetrical species **17**. Unfortunately, infrared spectra and conductivity measurements do not assist greatly in identifying the species other than to establish that only terminal isocyanides are present and that the solution mixture (containing five species over a wide range of stoichiometries) is weakly conducting. After the addition of 1 equiv of CNMe, there is still a significant amount of starting material present with the additional compounds **14**, **15**, **16**, and **17** present in the approximate respective ratios 1.00:0.40:0.25:0.20. Upon further CNMe addition the starting material **2** is consumed while the ratio of products remains essentially the same until the consumption of **2** is complete, after which time the mixture is converted to the tetrakis(isocyanide) species **13c**. The $^{31}P\{^1H\}$ NMR spectrum after the addition of approximately 1.3 equiv of CNMe is shown in Figure 3, where both 1:1 adducts **14** and **15**, the 2:1 adducts **16** and **17**, and the 4:1 adduct **13c** are visible. Three possible structures seem reasonable for the symmetrical species **17**, as shown in VI–VIII. We consider the fourth possibility, a dicationic species, $[Rh_2(CNMe)_2(\mu\text{-HFB})(DPM)_2]^{2+}$, unlikely owing to the resulting electron deficiency of the metals, and once again, attempts to isolate such a species by addition of Ag^+ to solutions of the 2:1 adducts failed. On the basis of steric grounds, one might expect structure VIII to be the most likely; however, based on the lower tendency for the iodo ligand to bridge two metals which are bonded to each other, it is difficult to explain why no analogous chloro-bridged species was observed in the reaction of 1 with CNMe. We suggest therefore that the symmetrical species **17** has the structure VI or VII. This is consistent with the lower tendency of these low-valent Rh complexes to dissociate I^- compared to Cl^-. Furthermore, structures VI and VII are rather analogous to that observed[24] for $[Rh_2(CN\text{-}t\text{-}Bu)_4(\mu\text{-HFB})(DPM)_2]^{2+}$. Species corresponding to structures I and II must dissociate halide before subsequent reaction with CNMe occurs to yield the unsymmetrical bis(isocyanide) species, since the metal having the coordinated CNMe group is an 18-electron center. Although we tried and failed to isolate such a species, as described earlier, this does not rule it out as a reactive intermediate. If as we suggest the iodo group on the Rh atom having the coordinated CNMe group is less likely to dissociate than Cl^-, then attack by a second CNMe group at this metal center is inhibited and so attack at the other metal center becomes competitive and we see both the unsymmetrical and the symmetrical 2:1 adducts (**16** and **17**, respectively). We are unable to assign the symmetrical species as either structure VI or VII. Clearly iodide dissociation is not totally inhibited since both **16** and **17** are in equilibrium and both react with further CNMe to give the 4:1 adduct $[Rh_2(CNMe)_4(\mu\text{-HFB})(DPM)_2][I]_2$. It is significant that this product has somewhat different spectral parameters than the chloro analogue, even though the cations are the same. This is consistent with out notion that significant ion pairing occurs, as judged by the conductivity data.[15]

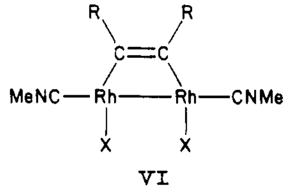

VI

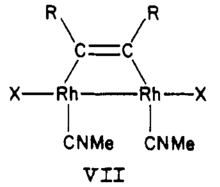

VII

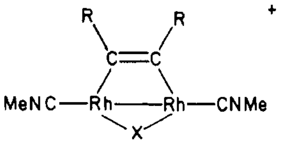

VIII

In order to determine the extent to which the nature of the bridging acetylene might influence the equilibria observed in the reactions of 1 and 2 and also to attempt to obtain further information about the structural details of the products in these reactions, we looked at the reaction of $[Rh_2Cl_2(\mu\text{-DMA})(DPM)_2]$ (**3**) with CNMe. Only one 1:1 adduct (**18**) is observed in the reaction of **3** with CNMe. On the basis of the position of the ^{1}H resonance for the CNMe group, it seems that this compound corresponds to the less abundant isomer obtained in the equivalent reactions with 1 and 2; we therefore assign it either structure II or III. Although this seems to be the least favorable situation since attack at the vacant site on Rh, adjacent to the coordinated acetylene ligand, should be unfavorable due to steric interactions with the methoxycarbonyl moiety, it should be noted that steric interactions in this product are minimized if the chloro group occupies the bridging site as in isomer III.

Only one, unsymmetrical 2:1 adduct (**19**) is obtained with compound **3**; this species is similar in its spectral parameters to the analogous products **12** and **16**. It is significant that no symmetrical product, analogous to **17**, is observed. This is consistent with the larger conductivity measurements obtained for the DMA-bridged species;[15] the only symmetrical 2:1 product was observed for the iodo ligand, and its presence was explained based on the lower tendency of I^- to dissociate from the complex.

As in all the previous reactions, addition of further CNMe leads to the formation of a 4:1 adduct, in this case $[Rh_2(CNMe)_4(\mu\text{-DMA})(DPM)_2]^{2+}$ (**20**). Again the conductivity of this species is low, but not unexpectedly so for such a species having Cl^- anions in a medium of low dielectric constant.

On the basis of the data given above for the CNMe reactions with compounds 1, 2, and 3 we propose Scheme I for these reactions. Although all three reaction sequences are closely related, there are subtle differences that arise as a consequence of the different halide or acetylene

Scheme I

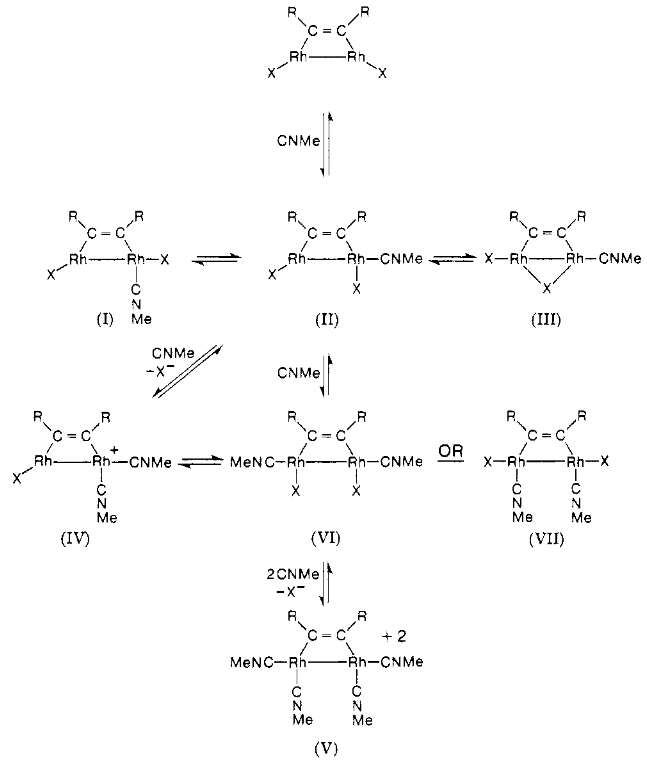

groups. For the HFB-bridged complexes two 1:1 adducts are obtained, of which the more abundant is proposed to correspond to structure I and the less abundant to III or a rapidly equilibrating mixture of isomers II and III. The higher abundance of isomer I for the iodo species may be related to the lower tendency of the iodo ligand to bridge the metals, which therefore reduces the abundance of isomer III. The fact that the 1:1, DMA-bridged product appears only as one isomer is believed to be due to structure III being favored owing to steric interactions between the CNMe group and the methoxycarbonyl groups on the acetylene. Reaction with a second equivalent of CNMe can occur either by halide dissociation to give structure IV or without halide dissociation to yield either VI or VII. The symmetrical species is observed only for the iodo complex, and this can be related to the lower tendency for I^- to dissociate compared to Cl^-. The 2:1 adducts react with 2 equiv of CNMe to yield the dicationic 4:1 adducts shown in structure V. No 3:1 adduct is observed. It is significant that, unlike the reactions of **1**, **2**, and **3** with CO and SO_2, the reactions with CNMe yield no products having bridging isocyanide groups.

Conclusions

The acetylene-bridged complexes $[Rh_2X_2(\mu\text{-}RC{\equiv}CR)(DPM)_2]$ (R = CF_3, X = Cl (**1**), I (**2**); R = CO_2Me, X = Cl (**3**)) react with CO and SO_2 via insertion into the Rh–Rh bond. This reaction with CO is one of the very few examples of CO insertion into a metal–metal single bond to give a "ketonic" carbonyl group.[4] In contrast, CNMe reacts with the above complexes to yield 1:1, 2:1, and 4:1 adducts, all of which contain terminal methyl isocyanide groups. No evidence of insertion into the metal–metal bond was observed with CNMe. Although these CNMe reactions, with the acetylene-bridged complexes, parallel those observed with the analogous carbonyl-bridged species $[Rh_2Cl_2(\mu\text{-}CO)(DPM)_2]$,[7] the reactions of compounds **1**, **2**, and **3** with CO and SO_2 differ significantly from those observed with both $[Rh_2Cl_2(\mu\text{-}CO)(DPM)_2]$ and $[Rh_2Cl_2(\mu\text{-}SO_2)(DPM)_2]$.[2,3,5] In no case was CO or SO_2 insertion into the Rh–Rh bonds of these latter two species observed as was the case for the acetylene-bridged analogues. This is possibly not surprising when we consider, for example, the product that would result from CO insertion into the Rh–Rh bond of $[Rh_2Cl_2(\mu\text{-}CO)(DPM)_2]$. This species would have two sp^2-hybridized carbonyl groups as diagrammed in IX. In this geometry (having Rh–C(O)–Rh angles of ca. 120° and Rh–C distances of ca. 2.00 Å) the nonbonded contact between the two carbonyl groups would be only ca. 2.00 Å —a distance which we feel is much too short for a nonbonded interaction of this sort. In contrast, there is much less contact between the bridging CO and the acetylenic carbons in the acetylene-bridged analogues (structure X); this separation is greater than 2.8 Å. Analogously short contacts would also be present in the products of either CO insertion into the Rh–Rh bond of the SO_2-bridged complex or SO_2 insertion into the CO-bridged complex and would presumably contribute to a destabilization of these products. It should be pointed out however that arguments based solely on repulsive van der Waals contacts cannot be the whole answer since a somewhat analogous species involving a bridging SO_2 group, two bridging methylthio groups, and no accompanying metal–metal bond ($[Fe_2(CO)_4(PMe_3)_2(\mu\text{-}SMe)_2(\mu\text{-}SO_2)]\cdot{}^1/_2Et_2O$) is known.[45] In this compound the Fe–S–Fe angles are only ca. 83–89°, resulting in acceptable S–S contacts of near 3.0 Å.

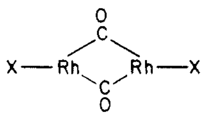

IX

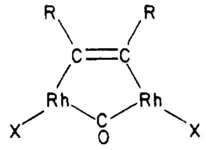

X

It seems therefore that whether or not reactivity at the metal–metal bond occurs in these binuclear group 8 metal complexes depends on the relative Lewis acidities of the metals and the incoming ligand (with the weaker Lewis acid CNMe failing to bridge the Rh–Rh bond in the present series) and on the nature of the bridging groups. It seems to us that complexes containing two carbonyls (or analogous groups such as SO_2, CH_2, CNR, etc.) that bridge two metals not bonded to each other should be severely destabilized owing to the resulting short nonbonded contacts.

Acknowledgment. We thank NSERC (Canada) and the University of Alberta for supports of this research and NSERC for a postdoctoral fellowship (B.W.H.).

Registry No. 1, 77590-00-2; **2**, 92345-50-1; **3**, 92345-51-2; **4**, 75503-68-3; **5**, 79272-86-9; **6**, 75503-67-2; **7**, 92365-77-0; **8**, 92365-78-1; **9**, 92365-79-2; **10**, 92345-52-3; **11**, 92345-53-4; **12a**, 92345-54-5; **12b**, 92345-64-7; **13a**, 92345-55-6; **13b**, 92345-66-9; **13c**, 92365-80-5; **14**, 92345-56-7; **15**, 92345-57-8; **16**, 92345-58-9; **17**, 92345-59-0; **18**, 92345-60-3; **19**, 92345-61-4; **20**, 92345-62-5; Rh, 7440-16-6.

Supplementary Material Available: Listings of the anisotropic thermal parameters, the derived hydrogen positions, the observed and calculated structure factor amplitudes for compound **12b** and a table of conductivity data for the reactions of compounds 1–3 with CNMe (24 pages). Ordering information is given on any current masthead page.

---

(45) Taylor, N. J.; Arabi, M. S.; Mathieu, R. *Inorg. Chem.* **1980**, *19*, 1740.